IEEE Access
Multidisciplinary | Rapid Review | Open Access Journal

Received February 2, 2019, accepted February 21, 2019, date of publication March 5, 2019, date of current version April 19, 2019.

Digital Object Identifier 10.1109/ACCESS.2019.2902977

Voltage Build-Up Analysis of Self-Excited Induction Generator With Multi-Timescale Reduced-Order Model

KAILIANG TENG[1,2], ZIGUANG LU[1], JUN LONG[1], YAODONG WANG[2], AND ANTHONY PAUL ROSKILLY[2]

[1]School of Electrical Engineering, Guangxi University, Nanning 530004, China
[2]Sir Joseph Swan Centre for Energy Research, Newcastle University, Newcastle upon Tyne NE1 7RU, U.K.

Corresponding author: Ziguang Lu (luzg@ gxu.edu.cn)

This work was supported in part by the National Natural Science Foundation of China under Grant 51567002, in part by the Natural Science Foundation of Guangxi Zhuang Autonomous Region, China, under Grant 2018GXNSFDA138008, and in part by the Project of Guangxi University Outstanding Post-Graduate Student Abroad under Grant T2040098001.

ABSTRACT Self-excited induction generator (SEIG) has received a lot of attentions for its increasing application in distributed generation systems with the essential feature of low cost. To analysis, the dynamic and transient performance of SEIG, several modifications of the mathematical models have been developed for improving the regulation of voltage and frequency. But these models are still complicated to be used in practice. Based on the transient equivalent circuit, a reduced-order model of SEIG with complex transformation in the two-phase stationary reference frame is realized for the transient analysis of voltage build-up. In this simplified model, the coefficients of the characteristic polynomial with multi-timescale time constants are proposed. Moreover, the physical interpretation of system transient behavior with the reconstructed time constants is established and visualized. Particularly, the upper and lower limits of the capacitance and speed for the SEIG with different parameters variation are simulated and analyzed respectively. The validation and the accuracy of the SEIG model are verified for the transient analysis of the voltage build-up. It is proved that the reduced-order model can be effectively used to insight the dynamic stability of SEIG voltage build-up with the multi-timescale.

INDEX TERMS Autonomous system, characteristic polynomial equations, complex coefficients, multi-timescale, self-excited induction generator, voltage build-up analysis.

I. INTRODUCTION

With increasing demand for the amounts of electricity from the potential distributed energy in wind, hydropower, biomass, and tidal, self-excited induction generator (SEIG) is becoming a popular dynamo which has the advantages of lower maintenance demands and relatively simplified controls in conjunction with the different prime movers for effective utilization of these renewable energy sources [1]. The challenges of using SEIG are the quality control of the power out, i.e. voltage and frequency when driven by the intermittent energy resources. Therefore, more attentions have been drawn on improving the voltage, frequency, and regulating the power quality of SEIG-based distributed generation system, especially its stabilization and the influence factors [2]–[5].

SEIG is commonly a kind of induction machine with squirrel cage or wound rotor [6]. The doubly fed induction generator (DFIG) is conveniently applied in variable speed operation, the permanent magnet synchronous generator (PMSG) has the value of the higher efficiency, but the SEIG is more attractive in small scale conversion system for the benefit of cost-effective, less maintenance, sturdiness, and durableness [7], [8]. Nevertheless, SEIG is a typical nonlinear system coupled with the complicated characteristic as high order, strong coupling, multivariable, and time varying, which limits further research on its dynamic and transient characteristic. Thus, further studies into the characteristics of SEIG is necessary, and the appropriate modeling methods needed to be provided to investigate the transient behavior

The associate editor coordinating the review of this manuscript and approving it for publication was Canbing Li.

and improve the voltage and frequency regulation of SEIG for the cost-effective utilization [9], [10].

Based on the well-known transformation method with reference-frame theory, the complexity of electric machine model can be reduced readily [11]. Although the rotor position-dependent variables in the induction machine can be both described by the static and synchronous rotating reference frame, parts of the cross-coupled term in the voltage and flux equations are still baffled the further development in the analysis and application. Compared to the generalized fifth-order model of linear magnetic system, an E-model concept of third-order model which ignored the transient characteristics is developed for describing large wind turbines to avoid the complete representation with the conventional complex transient model [12]. By neglecting the quantities of stator resistant and differential item of stator flux, a third model of DFIG with electromotive force is represented to capture the main electro-mechanical dynamics which similar to the fifth-order model in the large power plants [13]. Additionally, a simple first-order model is discussed in the literature for designing controller with the assumption that the response of current control is faster than the transient variation of generator stability, but the major disadvantage of this model is hard to further reflect the transient characteristics of power system. Seventh-order model of cascaded doubly fed induction generator (CDFG) is simplified by neglecting the electric transients and flux magnitude of rotor [14], and the full order model of double-cage induction generator (DCIG) is reduced by neglecting the transient of fluxes in two sequence equations [15], but the integrity of dynamic characteristic and stability in the generator are both compromised.

Prior to the advent of effective tool, the full order model of three phase cage induction generator without reference-frame transformation is developed by several six-order matrices and state space equations, but the complexity of analysis procedure and computational process are considerable [16]. A modified polynomial equation of induced electromotive force (EMF) versus reactance characteristic with six-order is presented to analysis SEIG system using linear search and binary search algorithms, and the lengthy derivations of design and development are avoided. However, based on the nodal admittance of the steady-state equivalent circuit to approximate the dynamics of SEIG system, the reduced-order model still suffered from the shortage of transient features [17]. A systematic comparison of the full model and the simplified model with linear magnetic is presented with the simulation and experiment, results confirmed that full model is more accurate than the simplified model, because the simplified model involved an approximation to the complex dynamic behavior [18]. The impedance equation of SEIG steady-state model with the graph theory is investigated to calculate the approximate value of SEIG stability boundary with differential evolution algorithm, but the corresponding relationship between the mechanism among inherent parameters of SEIG system and the stability are not described in detail [19]. A state-space linearized model and its characteristic polynomial of SEIG transient equivalent circuit with magnetic saturation is established in compact form. The eigenvalues of the linearized models and the full models are calculated to compare for the differences. However, the corresponding model of system and its computation is still intricate [20].

The regulation of voltage and the stability in the voltage build-up process of SEIG are sensitively affected by excitation capacitance, rotor speed, and the variation of motor parameters and load [21], [22]. It is essential to ensure, the appropriate value of capacitor is basic essential for the SEIG-based system to self excitation [23], [24], which provided the lagging magnetizing reactive power to maintain the air gap flux linkage of induction machine between the stator and rotor [25]. In order to keep the terminal voltage constant in the SEIG system, a Newton-Raphson approach with a cubic law equation which roughly fitted the experimental measurements curve is implemented to calculate the appropriate values of capacitor [26]. Owing to the advanced static compensator (STATCOM) and the developed mathematical model with proposed controller, the required reactive power is adjusted to maintain the terminal voltage of SEIG system [27]; and the capability of the low voltage ride through (LVRT) for integration of wind turbines into the grid is enhanced [28]. Meanwhile, the voltage and frequency of SEIG-based system with three renewable sources can be controlled well by integrating a converter with adaptive sliding mode control (ASMC) [29].

The full order of SEIG system which can be reduced by the Hurwitz criterion in state-space with six-order matrix is derived to calculate the range of capacitor values and the eigenvalues of stability for self-excitation [30]. Furthermore, the equivalent transfer function with complex root locus rules is discussed to reveal the dynamics of the balanced three-phase SEIG system [31]. Nevertheless, these reduced-order models of SEIG have less physical interpretation for further revealing the inherent transient and dynamic characteristics of the system. Although some low-order models were developed and tested in order to replace the high-order and transient models to reduce computation time, the physical meaning problem related to the dynamic processes and the parameters variation with spontaneous self-excitation are lost in these simplified models. Therefore, it is necessary to carry out further study into this area.

The aim of this research is to develop a more compact reduced-order model with four reconstructed time constants to insight more transient behaviors of SEIG system, reduce the complexity for calculating the excitation capacitance range, and evaluate the relation of the parameter variations of induction machine and the stability. Meanwhile, the characteristic polynomial of SEIG state space equation can be decoupled with the multi-timescale time constants for comprehension and physical interpretation. Finally, the proposed strategy and visualized signal flow diagram can provide a concise tool for the analysis of the dynamic characteristics of SEIG system.

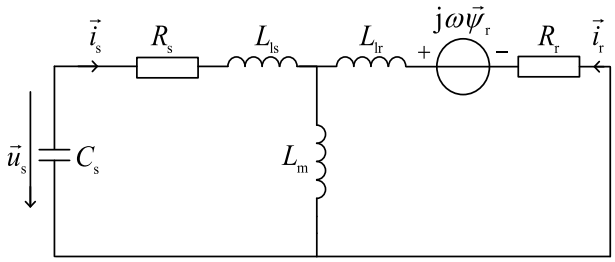

FIGURE 1. Transient equivalent circuit of SEIG.

II. FUNDAMENTAL ANALYSIS

A. REDUCED-ORDER SEIG MODEL

Based on the reference-frame theory [11], the space vector theory [32], and the advanced modeling technique with complex transformation [33], a compact mathematics model of three phase symmetric induction machine in the two-phase stationary reference frame is established by neglecting the effects of hysteresis, eddy currents, and magnetic saturation. Among them, the cross-coupled term of the voltage and flux equation in the model can be eliminated effectively.

$$\begin{cases} R_s\vec{i}_s + \dfrac{d\vec{\psi}_s}{dt} = \vec{u}_s \\ R_r\vec{i}_r + \dfrac{d\vec{\psi}_r}{dt} - j\omega\vec{\psi}_r = 0 \end{cases} \tag{1}$$

$$\begin{cases} L_s\vec{i}_s + L_m\vec{i}_r = \vec{\psi}_s \\ L_r\vec{i}_r + L_m\vec{i}_s = \vec{\psi}_r \end{cases} \tag{2}$$

where stator voltage vector $\vec{u}_s$ of asynchronous motor, stator current vector $\vec{i}_s$, rotor current $\vec{i}_r$, stator flux vector $\vec{\psi}_s$, and rotor flux vector $\vec{\psi}_r$ are defined by:

$$\begin{cases} \vec{u}_s = u_{s\alpha} + ju_{s\beta} \\ \vec{i}_s = i_{s\alpha} + ji_{s\beta} \\ \vec{i}_r = i_{r\alpha} + ji_{r\beta} \\ \vec{\psi}_s = \psi_{s\alpha} + j\psi_{s\beta} \\ \vec{\psi}_r = \psi_{r\alpha} + j\psi_{r\beta} \end{cases} \tag{3}$$

Based on the instantaneous power theory, the imaginary notation j is a complex number that reflecting the orthogonal relationship of motor state variables and revealing the physical meaning of reactive power in electrical systems [34]. With the assumed direction of stator and rotor current, the transient equivalent circuit of SEIG which composed of shunt excitation capacitor under no-load is shown in Fig. 1. where the leakage inductance L_{ls} and L_{lr} are defined as:

$$\begin{cases} L_{1s} = L_s - L_m \\ L_{1r} = L_r - L_m \end{cases} \tag{4}$$

As the direction of positive current for the transient equivalent circuits depicted in the Fig. 1, the dynamic differential equation of excitation capacitor with complex coefficient in the two-phase static reference frame can be derived as:

$$\vec{i}_s = -C_s\frac{d\vec{u}_s}{dt} \tag{5}$$

By substituting the stator flux vector and the rotor current vector from (2) to (1), the compact differential equations of induction motor are yield as:

$$\begin{cases} R_m\vec{i}_s + \sigma L_s\dfrac{d\vec{i}_s}{dt} - K_r(\dfrac{1}{\tau_r} - j\omega)\vec{\psi}_r = \vec{u}_s \\ -K_rR_r\vec{i}_s + \dfrac{d\vec{\psi}_r}{dt} + (\dfrac{1}{\tau_r} - j\omega)\vec{\psi}_r = 0 \end{cases} \tag{6}$$

where, $R_m = R_s + K_r^2R_r$, $\sigma = 1 - L_m^2/(L_sL_r)$, $K_r = L_m/L_r$, $\tau_r = L_r/R_r$.

B. MULTI-TIMESCALE SEIG MODEL

From reduced-order model (7) and the coefficients of the characteristic polynomial (9), it can be seen that the real and imaginary coefficients are both comprised with the inherent parameters of the SEIG system. Furthermore, the imaginary coefficients are directly related to the angular velocity of the generator rotor.

The time constants of excitation capacitor and rotor time are inherent in SEIG. With the transient stator time constant τ_s' and equivalent resistance R_m were obtained from [35], the transient air gap time constant τ_m' and transient capacitance time constant τ_c is further defined in this research. As a result, a whole time constant table of SEIG is listed in Table 1.

TABLE 1. Time constant.

Section	Component	Resistance	Time constant
Terminal	C_s	$R_m = R_s + (\dfrac{L_m}{L_r})^2 R_r$	$\tau_c = R_mC_s$
Stator	$L_s' = \sigma L_s$	$R_m = R_s + (\dfrac{L_m}{L_r})^2 R_r$	$\tau_s' = \dfrac{L_s'}{R_m}$
Air gap	$L_m' = \dfrac{\sim_m}{L_r}$	$R_m = R_s + (\dfrac{L_m}{L_r})^2 R_r$	$\tau_m' = \dfrac{L_m'}{R_m}$
Rotor	L_r	R_r	$\tau_r = \dfrac{L_r}{R_r}$

With the proposed four time constants in the Table 1, the differential equations of excitation capacitor in (5) and induction motor model (6) can be both rewritten as

$$\vec{i}_s = -\frac{\tau_c}{R_m}\frac{d\vec{u}_s}{dt} \tag{7}$$

$$\begin{cases} \vec{i}_s + \tau_s' \dfrac{d\vec{i}_s}{dt} - \dfrac{\tau_m'}{L_m}\left(\dfrac{1}{\tau_r} - j\omega\right)\vec{\psi}_r = \dfrac{1}{R_m}\vec{u}_s \\ -\dfrac{L_m}{\tau_r}\vec{i}_s + \dfrac{d\vec{\psi}_r}{dt} + \left(\dfrac{1}{\tau_r} - j\omega\right)\vec{\psi}_r = 0 \end{cases} \tag{8}$$

Taking the stator voltage vector, stator current vector and rotor flux vector as state variables from (7) and (8), the reduced-order model of SEIG system with four time constants in time domain is derived as:

$$\frac{d}{dt}\begin{bmatrix} \vec{u}_s \\ \vec{i}_s \\ \vec{\psi}_r \end{bmatrix} = \begin{bmatrix} 0 & -\dfrac{R_m}{\tau_c} & 0 \\ \dfrac{1}{R_m\tau_s'} & -\dfrac{1}{\tau_s'} & \dfrac{\tau_m'}{\tau_s' L_m}\left(\dfrac{1}{\tau_r} - j\omega\right) \\ 0 & \dfrac{L_m}{\tau_r} & -\dfrac{1}{\tau_r} + j\omega \end{bmatrix} \begin{bmatrix} \vec{u}_s \\ \vec{i}_s \\ \vec{\psi}_r \end{bmatrix} \tag{9}$$

Once there is not external voltage or current input to the build-up process of voltage, the model of SEIG system can be regarded as the autonomous system to analysis. Therefore, according to the stability criterion of the autonomous system [30], the solution of SEIG characteristic polynomial equation can be written as

$$\begin{aligned} |sI - A| = a_0 + jb_0 + (a_1 + jb_1)s \\ + (a_2 + jb_2)s^2 + (a_3 + jb_3)s^3 \end{aligned} \tag{10}$$

where, the real and imaginary coefficients of SEIG characteristic polynomial equation are:

$$\begin{aligned} a_0 &= \frac{1}{\tau_r}\left(\frac{1}{\tau_c \tau_s'}\right) \\ b_0 &= -\omega\left(\frac{1}{\tau_c \tau_s'}\right) \\ a_1 &= \frac{1}{\tau_c \tau_s'} + \frac{1}{\tau_r}\left(\frac{1}{\tau_s'} - \frac{\tau_m'}{\tau_s' \tau_r}\right) \\ b_1 &= -\omega\left(\frac{1}{\tau_s'} - \frac{\tau_m'}{\tau_s' \tau_r}\right) \\ a_2 &= \frac{1}{\tau_s'} + \frac{1}{\tau_r} \\ b_2 &= -\omega \\ a_3 &= 1 \\ b_3 &= 0 \end{aligned} \tag{11}$$

With the sufficient and necessary conditions of Routh stability criterion which are extended in the complex field, the critical analytical solution for the upper and lower limits of the capacitance in SEIG system can be figured out directly by the time constant of capacitor in (10). Furthermore, the simplified coefficients of characteristic polynomial can be all represented by the four defined time constants. It is worth noting that, the real and imaginary parts of each polynomial coefficient are both containing the identical constant term at the same time, such as a_1 and b_1 both include the time constants of τ_s' , τ_m' , and τ_r , as well as a_0 and b_0 containing τ_c and τ_s' . The real part of the characteristic polynomial is independent to the rotor speed, whereas the imaginary part on the contrary. In the same order of the time scale, the same cross-coupled term of the different time constant is revealing the physical mechanism of the rotation between the rotor and stator, which interpreting the basic essential of SEIG voltage build-up. Thus, the signal flow diagram of SEIG transient performance with the multi-timescale time constants is described in Fig. 2.

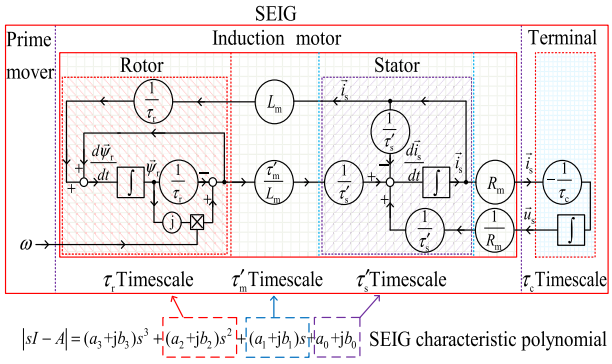

FIGURE 2. Multi-timescales signal flow diagram of SEIG.

From Fig. 2, the detailed multi-timescale signal flow graph is visualized with the four time constants and the characteristic polynomial. With the mechanical energy from the prime mover input to the rotor, the stator current of induction motor is drawn from the terminal excitation capacitor to create transient air gap flux linkage at first. Then, the raised stator current is feedback to strengthen the flux linkage of rotor. Finally, the stator current would be established continuously through the rotating flux linkage of rotor The positive feedback loop of stator current is reinforced by the terminal excitation capacitor and rotor flux linkage, which reveals the essential interpretation of SEIG voltage build-up. With the proposed signal flow diagram, the complexity for analyzing the critical transient stability of SEIG is reduced. At the same time, the effective relation for interpreting the physical significance of the proposed SEIG model and the polynomial coefficient expression is also characterized in Fig. 2, which will benefit for improving the voltage and frequency regulation of SEIG in further utilization.

C. NUMERICAL CASE STUDY

In order to investigate the relationship for the variation of different time constants with the stability boundary of SEIG voltage build-up process, a sample calculation of SEIG with no load are developed in MATLAB R2017b (MATLAB R2017b, MathWorks, Natick, MA, USA).

For comparing and verifying the correctness and the accuracy of the proposed reduced-order SEIG model, the configuration of induction machine which calculated in this case study is the same as [36]–[38]. Specify parameters are summarized in Table 2.

TABLE 2. SEIG parameters.

Parameters (Units)	Value
Rated voltage (V)	380
Rated current (A)	5
Power (kW)	2.2
Stator resistance (Ω)	2.8
Rotor resistance (Ω)	3.2
Stator leakage inductance (H)	0.0109
Rotor leakage inductance (H)	0.0109
Mutual inductance (H)	0.3754
Pole pairs	2
Frequency (Hz)	50
Rated speed (rpm)	1500
(Mechanical angular velocity (rad/s))	(157.08)

The characteristic of the mutual inductance and the excitation current is a nonlinear relationship. In the initial transient process of SEIG voltage built-up, the excitation current is far less than the rated value and the mutual inductance has not reached the saturation region yet. Therefore, the mean value of the mutual inductance is set to 0.3754 H in this study. In order to analyze the stability of SEIG voltage build-up process, it is assumed that the generator is driven by a prime mover at different steady speed to calculate the corresponding critical values.

III. RESULTS AND DISCUSSION

According to the sufficient and necessary conditions of Routh stability criterion within the complex field from (6) to (10) above, the critical lower and upper limit results of capacitance for SEIG voltage build-up with rated speed are obtained by the proposed multi-timescale reduced-order model and compared to the results from [36]–[38].

According to the methods in [36]–[38] which are based on the six-order state-space model and its complex higher-order polynomials, the procedure for solving the lower and upper limits of the capacitance would be intricate and time consuming by comparing to the proposed three-order model and strategy. From the results shown in Table 3, it can be seen that the accuracies of the results from the other models in [36]–[38] are from 0.015 % to 2.59 %. The more precise results from this research showed that, the effectiveness of the reduced-order model for analyzing the transient stability of SEIG voltage build-up is proved

In order to investigate the sensitivity for the accuracy of results in Table 3, the simulation of SEIG three-phase output voltage with different critical upper and lower limits of the capacitance in the time domain are shown in Fig. 3 and Fig. 4.

With the residual magnetism in the rotor, the initial three phase output voltage of SEIG operating at rated mechanical angular velocity is mainly determined by excitation capacitance. The initial output voltage with critical lower capacitance is 91 V, as well as 19 V with critical upper capacitance.

TABLE 3. Comparison of results.

Methods	Lower limit of capacitance (μF)	Error (%)	Upper limit of capacitance (μF)	Error (%)
[36]	26.3	0.015	1900	2.59
[37]	26.3	0.015	1949	0.015
[38]	26.28	0.092	1947	0.12
This study	26.3041	0.00019	1949.2959	0.0000015

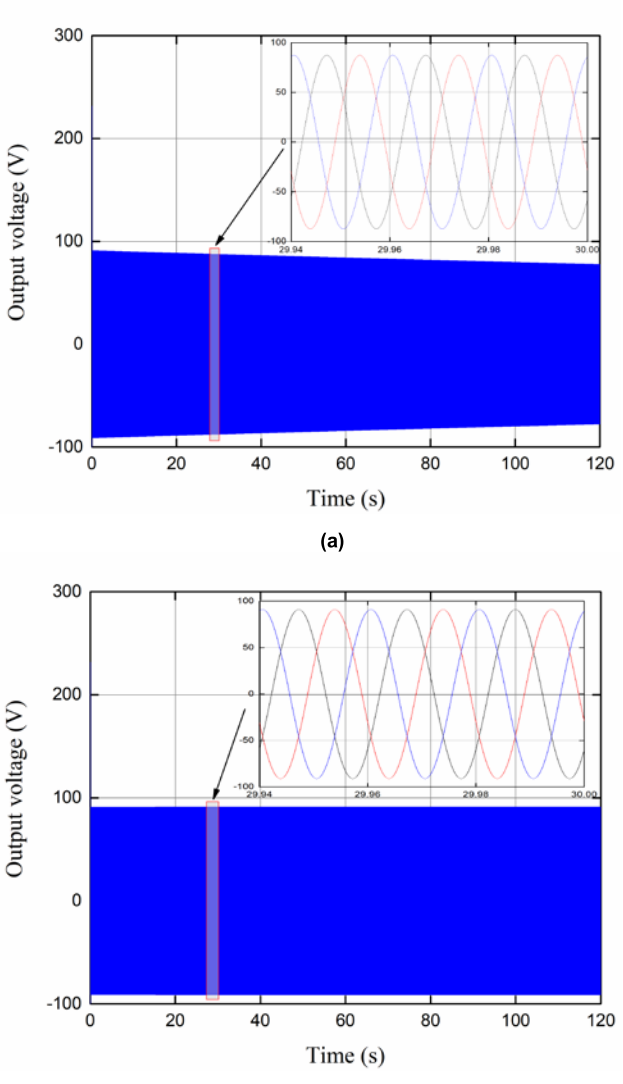

FIGURE 3. Simulations of SEIG three-phase output voltage with different lower limit of capacitance: (a) 26.3 uF, (b) 26.3041 uF.

Based on the well-known stability theory, the three-phase output voltages of SEIG with terminal excitation capacitance will maintain a constant value. In contrast to other methods, the calculated results from the simulation of SEIG voltage build-up process are more accurate with the proposed strategy as seen in Fig. 3(b) and Fig. 4(b). Once the capacitance

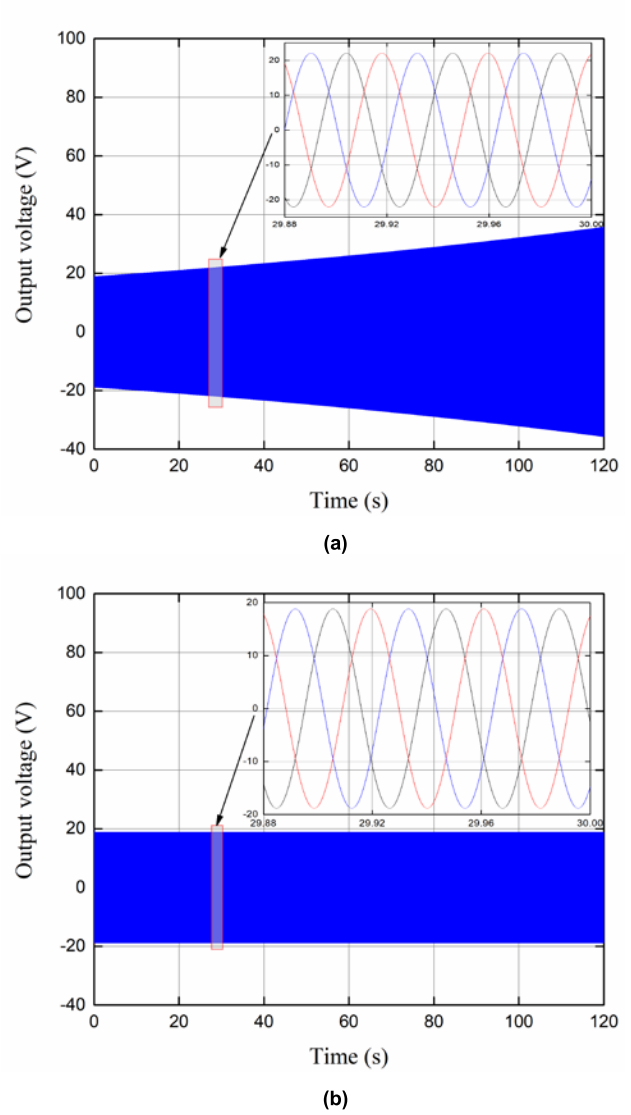

FIGURE 4. Simulations of SEIG three-phase output voltage with different upper limit of capacitance: (a) 1949 uF, (b) 1949.2959 uF.

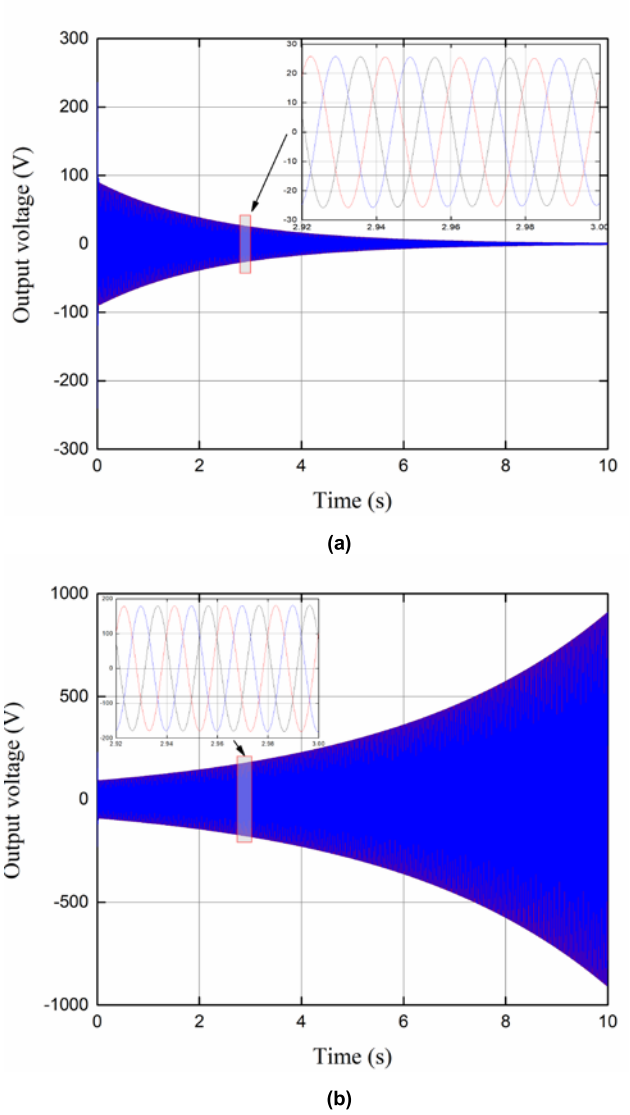

FIGURE 5. Simulations of SEIG three-phase output voltage with different lower limit of capacitance: (a) 25 uF, (b) 27 uF.

value is changed slightly from the real critical value in other models, the final transient performances of SEIG initial output voltage are diverged to 77 V and 36 V within the 120 seconds results of simulation respectively, as shown in Fig. 3(a) and Fig. 4(a).

To further verify the accuracy of the results with the proposed reduced-order model, simulations of variations around the critical upper and lower limits of the capacitance are given in the following Fig. 5 and Fig. 6. When the excitation capacitance is out of the critical range in Table 3, the three-phase output voltages of SEIG system are decayed in Fig. 5(a) and Fig. 6(b), which cause the operation of SEIG is failed to start in the end.

Reversely, as shown in Fig. 5(b) and Fig. 6(a), as long as the excitation capacitances are larger than the critical lower capacitance and smaller than the critical upper capacitance respectively, the steady voltage build-up process of SEIG is guaranteed. Notice that, this study is focus on the initial transient state of voltage built-up process, the excitation current of SEIG is far less than the rated current, as well as the mutual inductance unreached the saturation region. Therefore, without the limitation of the magnetic saturation effect and the iron losses, the final output voltages of SEIG will be increasing continuously, as shown in Fig. 5(b).

With the instantaneous power theory, the results of simulations from Fig. 3 to Fig. 6 show the real part of polynomial coefficient in (10) involves the amplitude dimension of the SEIG stability boundary, as well as the imaginary part is closely correlated with the phase dimension. For further revealing the relationship of the proposed time constants and the coefficients of characteristic polynomial,

TABLE 4. Results of time constants and real coefficients.

Symbol	Time constants and Coefficients	Results
τ_c	Transient capacitance time constant	0.0001531
τ_s'	Transient stator time constant	0.003692
τ_m'	Transient air gap time constant	0.06266
τ_r	Rotor time constant	0.1207
a_1	First order real coefficient	14654930.9511
a_2	Second order real coefficient	1770204.134
a_3	Third order real coefficient	279.1679

specify calculation results from (10) and Table 2 are shown in Table 4.

From Table 4, it can be seen that the time constant of excitation capacitance is 24 times fast than the stator, and the stator time constant is 17 times fast than the air gap, as well as the rotor is 2 times slower than air gap. Similar to the real coefficients of characteristic polynomial, each part of the time constant is one magnitude smaller than the other, both representing a similar gradient relation of multi-timescale.

In Table 1, the coefficients of the characteristic polynomials can be represented by the four time constants in (10). Therefore, the analysis for the transient stability of SEIG voltage build-up can be simplified to the four time constants. Finally, the critical upper and lower capacitance of SEIG is just related to the terminal capacitor time constant. As comparison between the calculated results of four time constants in Table 4, the respond time of capacitance time constant is shortest one. As a result, the multi-timescale relation of the time constants reveals that the value of excitation capacitance has the most significant impact on the three-phase output voltage of SEIG system. Particularly those accurate critical values of the excitation capacitance are crucial for the stability analysis of SEIG voltage build-up process, which are shown in Fig. 3 to Fig. 6.

Table 1 shown that, the other time constants are combined with the inherent parameters of induction motor. To analyze the influence on the variation of motor parameters, the charts of critical excitation capacitance with different angular velocity are presented in Fig. 7 to Fig. 9.

It is noted that, while the value of excitation capacitance is designed between the curve of the upper and lower capacitance, the instability of the SEIG self-excitation is eliminated. Therefore, the trends for analyzing the stability boundary of SEIG are developed by the changing variations of motor parameter around 50 percent. As depicted in the Fig. 7, the red line indicates the performance for the rated resistance of the motor, and the other lines related to the

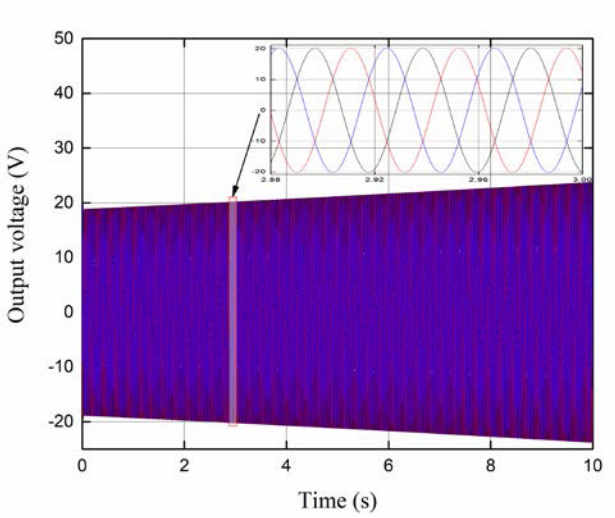

(a)

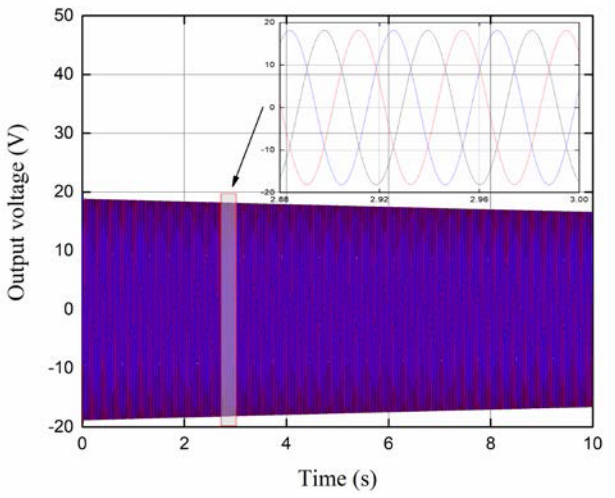

(b)

FIGURE 6. Simulations of SEIG three-phase output voltage with different upper limit of capacitance: (a) 1948 uF, (b) 1950 uF.

value of resistance increases and decreases 50%. As the results from Fig. 7(a), the peak of upper critical capacitance is sensitive to the variation of stator resistance, but the critical lower capacitance is independent from it. Unlike the influence of stator resistance, the variation of rotor resistance changes the angular velocity of the upper capacitance in Fig. 7(b).

According to the variation of the stator and rotor leakage inductance, the results of the Fig. 8(a) and Fig. 8(b) are almost the same. Therefore, the influence of leakage inductance variation is insensitive.

As the curve depicted in Fig. 9, the lines of the lower capacitance and the upper capacitance are both influenced by the mutual inductance. Moreover, the lower angular velocity of critical capacitance is also sensitive to the mutual inductance. And, more remarkably, there are some lower speed requirements in the Fig. 7 to Fig. 9 for building up the voltage of SEIG system. Under the lower speed,

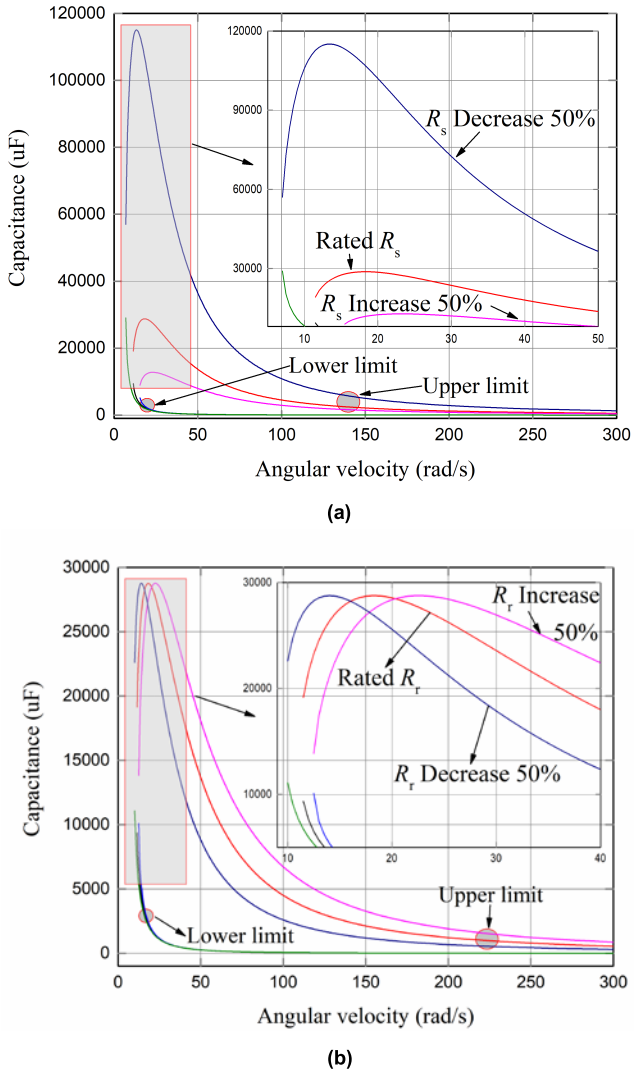

FIGURE 7. Lower and upper limit of capacitance with the variation of resistance of SEIG at different angular velocity: (a) stator resistance variation, (b) rotor resistance variation.

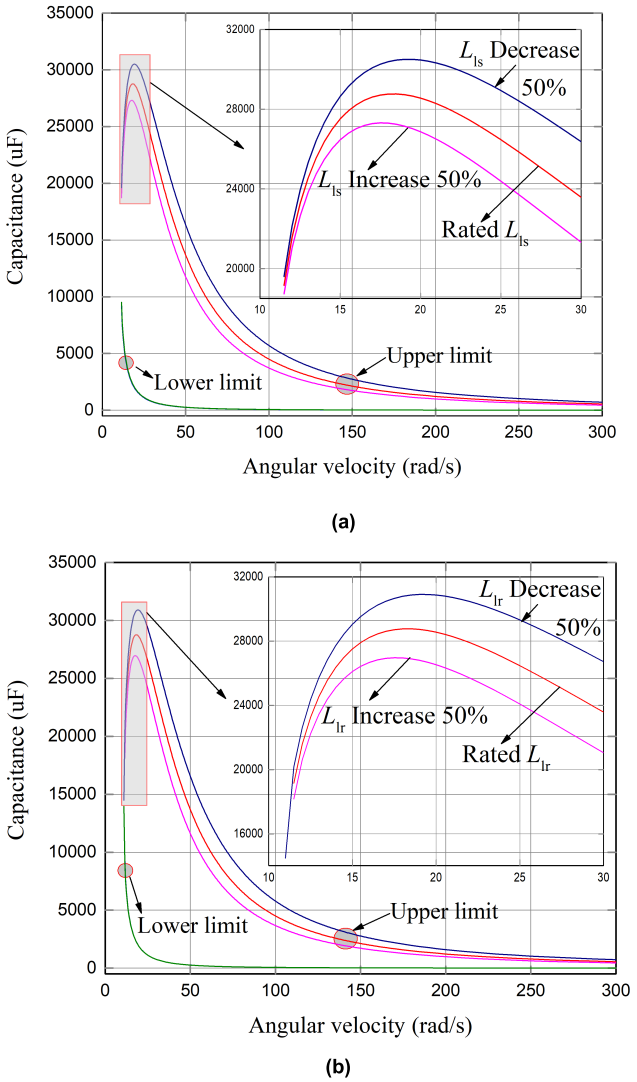

FIGURE 8. Lower and upper limit of capacitance with the variation of leakage inductance of SEIG at different angular velocity: (a) stator leakage inductance variation, (b) rotor leakage inductance variation.

the operation of SEIG system is failed with any excitation capacitance.

To summarize, the dynamic process of SEIG voltage build-up with different time scales are presented and compared, with insight of the regularity and physical concept of SEIG with multi-timescale constants. Furthermore, the efficiency and the accuracy analysis of SEIG with the reduced-order model are verified by the calculation and simulations.

IV. CONCLUSIONS

This paper presents a novel strategy for reducing the order of SEIG model to further insight the dynamic performance of the voltage build-up process. Main contributions and conclusions can be drawn as follows:

(1) A three-order of SEIG state equation without load is proposed and verified. The complexity of computation for analyzing the transient stability process of SEIG voltage build-up is reduced.

(2) Decouple the polynomial coefficients of characteristic equation with the four reconstructed time constants in multi-timescale. The relation between each time constants and the real coefficients of characteristic equation are analyzed and compared.

(3) The precise boundary curve for determining the lower and upper limit of SEIG capacitance are given with the angular velocity from zero to rated value, which is convenient for optimizing the cost-effective excitation capacitor to stabilize the three-phase output voltage.

(4) The detailed signal flow diagram of reduced-order model with four timescale constants is visualized, and the mechanism and physical significance is further interpreted for boosting the scope of the SEIG transient behavior. The results show that the proposed strategy is an effective

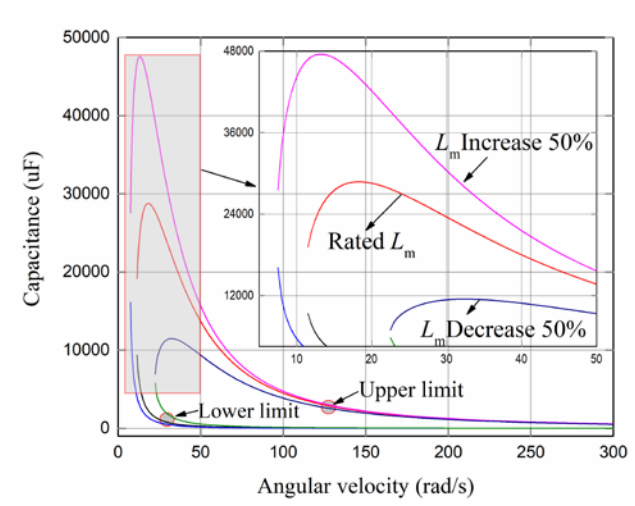

FIGURE 9. **Lower and upper limit of capacitance for the variation of mutual inductance with angular velocity.**

tool for designing and evaluating the performance of SEIG system.

REFERENCES

[1] S. Chatterjee and S. Chatterjee, "Review on the techno-commercial aspects of wind energy conversion system," *IET Renew. Power Gener.*, vol. 12, no. 14, pp. 1581–1608, Oct. 2018.

[2] R. E. Raj, C. Kamalakannan, and R. Karthigaivel, "Genetic algorithm-based analysis of wind-driven parallel operated self-excited induction generators supplying isolated loads," *IET Renew. Power Gener.*, vol. 12, no. 4, pp. 472–483, Mar. 2018.

[3] U. K. Kalla, B. Singh, and S. S. Murthy, "Green controller for efficient diesel engine driven single-phase SEIG using maximum efficiency point operation," *IEEE Trans. Ind. Electron.*, vol. 64, no. 1, pp. 264–274, Jan. 2017.

[4] A. K. K. Giri, S. R. Arya, R. Maurya, and B. C. Babu, "Power quality improvement in stand-alone SEIG-based distributed generation system using Lorentzian norm adaptive filter," *IEEE Trans. Ind. Appl.*, vol. 54, no. 5, pp. 5256–5266, Sep./Oct. 2018.

[5] U. K. Kalla, B. Singh, and S. S. Murthy, "Slide mode control of micro-grid using small hydro driven single-phase SEIG integrated with solar PV array," *IET Renew. Power Gener.*, vol. 11, no. 11, pp. 1464–1472, Sep. 2017.

[6] G. K. Singh, "Self-excited induction generator research—A survey," *Electr. Power Syst. Res.*, vol. 69, nos. 2–3, pp. 107–114, 2004.

[7] F. Blaabjerg and K. Ma, "Wind energy systems," *Proc. IEEE.*, vol. 105, no. 11, pp. 2116–2131, Nov. 2017.

[8] H. Polinder, J. A. Ferreira, B. B. Jensen, A. B. Abrahamsen, K. Atallah, and R. A. McMahon, "Trends in wind turbine generator systems," *IEEE J. Emerg. Sel. Topics Power Electron.*, vol. 1, no. 3, pp. 174–185, Sep. 2013.

[9] K. K. Raj and R. S. Rao, "Analysis of induction generators and advanced power electronic converters for wind energy conversion technology," *Proc. IEEE Asia Pacific Conf. Postgraduate Res. Microelectron. Electron. (PrimeAsia)*, Visakhapatnam, India, 2013, pp. 83–88.

[10] B. Novakovic, Y. Duan, M. G. Solveson, A. Nasiri, and D. M. Ionel, "From wind to the electric grid: comprehensive modeling of wind turbine systems," *IEEE Ind. Appl. Mag.*, vol. 22, no. 5, pp. 73–84, Sep./Oct. 2016.

[11] P. C. Krause, O. Wasynczuk, and S. D. Sudhoff, *Analysis of Electric Machinery and Drive Systems*. Hoboken, NJ, USA: Wiley, 2013, pp. 86–114.

[12] Z. Saad-Saoud and N. Jenkins, "Simple wind farm dynamic model," *IEE Proc.–Gener., Transmiss. Distrib.*, vol. 142, no. 5, pp. 545–548, Sep. 1995.

[13] K. Elkington and M. Ghandhari, "Comparison of reduced order doubly fed induction generator models for nonlinear analysis," *IEEE Electr. Power Energy Conf. (EPEC)*, Montreal, QC, Canada, 2009, pp. 1–6.

[14] R. Sadeghi, S. M. Madani, M. Agha-kashkooli, and M. Ataei, "Reduced-order model of cascaded doubly fed induction generator for aircraft starter/generator," *IET Electr. Power Appl.*, vol. 12, no. 6, pp. 757–766, Jul. 2018.

[15] A. Rolán, F. C. López, S. Bogarra, L. Monjo, and J. Pedra, "Reduced-order models of squirrel-cage induction generators for fixed-speed wind turbines under unbalanced grid conditions," *IEEE Trans. Energy Convers.*, vol. 31, no. 2, pp. 566–577, Jun. 2016.

[16] A. Alfarhan, S. M. Gadoue, B. Zahawi, M. Shalaby, and M. A. Elgendy, "Modelling of magnetizing inductance saturation in self-excited induction generators," in *Proc. IEEE 16th Int. Conf. Environ. Electr. Eng. (EEEIC)*, Florence, Italy, 2016, pp. 1–6.

[17] K. Arthishri, K. Anusha, N. Kumaresan, and S. Senthil Kumar, "Simplified methods for the analysis of self-excited induction generators," *IET Electr. Power Appl.*, vol. 11, no. 9, pp. 1636–1644, Nov. 2017.

[18] O. Kiselychnyk, M. Bodson, and J. Wang, "Comparison of two magnetic saturation models of induction machines and experimental validation," *IEEE Trans. Ind. Electron.*, vol. 64, no. 1, pp. 81–90, Jan. 2017.

[19] D. Samajpati and S. N. Mahato, "Graph theory based performance analysis of three-phase self-excited induction generator using differential evolution," in *Proc. Int. Conf. Electr. Power Energy Syst. (ICEPES)*, Bhopal, India, 2016, pp. 519–526.

[20] O. Kiselychnyk, M. Bodson, and J. Wang, "Linearized state-space model of a self-excited induction generator suitable for the design of voltage controllers," *IEEE Trans. Energy Conversion.*, vol. 30, no. 4, pp. 1310–1320, Dec. 2015.

[21] D. Wang and X. M. Yuan, "Interaction analysis between induction motor loads and STATCOM in weak grid using induction machine model," *J. Modern Power Syst. Clean Energy.*, vol. 6, no. 1, pp. 158–167, Jan. 2018.

[22] A. Sharma and G. Kaur, "Assessment of capacitance for self-excited induction generator in sustaining constant air-gap voltage under variable speed and load," *Energies*, vol. 11, no. 10, pp. 2509–2525, Oct. 2018.

[23] S. Paliwal, S. Kumar Sinha, and Y. Kumar Chauhan, "Performance optimization of self excited induction generator: a state of art," in *Proc. Recent Develop. Control, Autom. Power Eng. (RDCAPE)*, Noida, India, 2017, pp. 416–420.

[24] W. E. Vanco, F. B. Silva, F. A. S. Goncalves, and C. A. Bissochi, "Evaluation of the capacitor bank design for self-excitation in induction generators," *IEEE Latin Amer. Trans.*, vol. 16, no. 2, pp. 482–488, Feb. 2018.

[25] K. A. Chinmaya and G. K. Singh, "Performance evaluation of multiphase induction generator in stand-alone and grid-connected wind energy conversion system," *IET Renew. Power Gener.*, vol. 12, no. 7, pp. 823–831, May 2018.

[26] D. Chermiti, N. Abid, and A. Khedher, "Voltage regulation approach to a self-excited induction generator: Theoretical study and experimental validation," *Int. Trans. Electr. Energy Syst.*, vol. 27, no. 5, pp. 2311–2322, May 2017.

[27] B. Singh, S. S. Murthy, and S. Gupta, "STATCOM-based voltage regulator for self-excited induction generator feeding nonlinear loads," *IEEE Trans. Ind. Electron.*, vol. 53, no. 5, pp. 1437–1452, Oct. 2006.

[28] M. I. Mosaad, "Model reference adaptive control of STATCOM for grid integration of wind energy systems," *IET Electr. Power Appl.*, vol. 12, no. 5, pp. 605–613, May 2018.

[29] U. K. Kalla, B. Singh, S. S. Murthy, C. Jain, and K. Kant, "Adaptive sliding mode control of standalone single-phase microgrid using hydro, wind, and solar PV array-based generation," *IEEE Trans. Smart Grid*, vol. 9, no. 6, pp. 6806–6814, Nov. 2018.

[30] M. Bodson and O. Kiselychnyk, "The complex Hurwitz test for the analysis of spontaneous self-excitation in induction generators," *IEEE Trans. Autom. Control.*, vol. 58, no. 2, pp. 449–454, Feb. 2013.

[31] A. Dòria-Cerezo and M. Bodson, "Design of controllers for electrical power systems using a complex root locus method," *IEEE Trans. Ind. Electron.*, vol. 63, no. 6, pp. 3706–3716, Jun. 2016.

[32] P. K. KovÃącs, *Transient Phenomena in Electrical Machines*, vol. 9, Budapest, Hungary: Elsevier, 1984.

[33] J. Holtz, "The representation of AC machine dynamics by complex signal flow graphs," *IEEE Trans. Ind. Electron.*, vol. 42, no. 3, pp. 263–271, Jun. 1995.

[34] Q. Zhong, "The ghost operator and its applications to reveal the physical meaning of reactive power for electrical and mechanical systems and others," *IEEE Access*, vol. 5, pp. 13038–13045, 2017.

[35] J. Holtz, "Sensorless control of induction motor drives," *Proc. IEEE*, vol. 90, no. 8, pp. 1359–1394, Aug. 2002.

[36] T. F. Chan, "Capacitance requirements of self-excited induction generators," *IEEE Trans. Energy Convers.*, vol. 8, no. 2, pp. 304–311, Jun. 1993.
[37] H. T. Li and Z. G. Lu, "Analysis of voltage build-up for self-excited induction generators based on Lyapunov stability theory," (in Chinese), *Trans. China Electrotech. Soc.*, vol. 29, no. 9, pp. 167–173, Sep. 2014.
[38] J. Li, X. Z. Wu, and H. F. Wang, "Voltage build-up analysis of loaded self-excited induction generators based on Hurwitz stability criterion," (in Chinese), *Proc. Chin. Soc. Electr. Eng.*, vol. 38, no. 10, pp. 3094–3101, May 2018.

KAILIANG TENG was born in Nanning, China, in 1982. He received the B.S. degree in electrical engineering and automation from the College of Electrical Information Engineering, Hunan University, Changsha, China, in 2006, and the M.S. degrees in control engineering from the School of Automation, Wuhan University of Technology, Wuhan, China, in 2010. He is currently pursuing the Ph.D. degree in automation of electrical power systems, where he is also a Senior Engineer. His current research interests include the advanced control of generator and renewable energy generation technology.

ZIGUANG LU received the B.S. and M.S. degrees in industrial electric automation and industrial automation from the University of Science and Technology Beijing (USTB), Beijing, China, in 1985 and 1988, respectively, and the Ph.D. degree in electrical engineering from Tsinghua University, Beijing, China, in 2004.

In 1988, he joined the School of Electrical Engineering, Guangxi University (GXU), Nanning, China. He is currently a Professor with the School of Electrical Engineering, GXU, and is also the Director and Founder of the Institute of Advanced Control and Intelligent Power. He has published more than 80 technical papers. His current research interests include motor drive systems, power electronic systems, and renewable energy generation technology.

JUN LONG received the B.S. and M.S. degrees in electrical engineering from Guangxi University (GXU), Nanning, China, in 1982.

In 1982, he joined the School of Electrical Engineering, Guangxi University (GXU), Nanning, China, where he is currently a Professor of the School of Electrical Engineering. He has published more than 50 technical papers. His current research interests include detection and control technology in power systems, distributed generation, and smart grid.

YAODONG WANG is currently a Senior Lecturer and a very active Researcher working on sustainable, clean and renewable energy with Newcastle University, U.K. He has 20 years' experience working on 24 research projects including: Miller Cycle petrol and diesel engines; Flameless Oxidation to reduce NOx emissions from gas turbine and power plant; biofuel petrol/diesel engine; biofuel trigeneration and cogeneration with energy storage; energy systems such as biomass/coal thermal power stations: coal and biomass combustion and gasification; organic Rankine cycle; renewable energy systems (wind solar; biomass, water/hydropower); thermal energy management in processing industries; and building energy saving using passive and active methods. He has published more than 150 papers in peer-reviewed journals (more than 70) and conference proceedings (more than 80). He is an Invited Reviewer for 12 international journals and the Section Chair for 10 international conferences. He has supervised and is supervising more than 30 research students (12 Ph.D. and 11 M.Phil. graduated).

ANTHONY PAUL ROSKILLY is the Chair of Marine Engineering, and is currently the Director of the Sir Joseph Swan Centre for Energy Research; the Associate Director of the National Centre for Energy Systems Integration; and the Associate Director of the Institute for Sustainability, Newcastle University. He has held a number of senior positions, as the Dean of Research for the Faculty of Science, Agriculture and Engineering; supporting and coordinating the research strategy and activity in association with 10 academic schools; and seven Research Centers and two Research Institutes. He has 30 years' experience in the design, control, and operational optimization of energy systems and currently manages a personal research team of more than 40 PDRAs and PGR students. He is a member of the Science Board of the Energy Storage Supergen Hub, the UK contact for the European Energy Research Alliance Joint Programmes for Energy Efficiency in Industrial Processes (EEIP), and an Associate Editor of *Applied Energy* (APEN).